

# **The isoleucine at position 118 in transmembrane 2 is responsible for the selectivity of xamoterol, nebivolol and ICI89406 for the human $\beta$ 1-adrenoceptor.**

Victor Jun Yu Lim<sup>1\*</sup>, Richard G W Proudman<sup>2\*</sup>, Stefania Monteleone<sup>1</sup>, Peter Kolb<sup>1#</sup>, Jillian G Baker<sup>2#</sup>

<sup>1</sup>Institute of Pharmaceutical Chemistry, Philipps-University Marburg, Marbacher Weg 6, 35032 Marburg, Germany

<sup>2</sup>Cell Signalling, School of Life Sciences, C Floor Medical School, Queen's Medical Centre, University of Nottingham, Nottingham, NG7 2UH, UK.

\*these authors contributed equally to this work

#joint corresponding authors

Correspondence to [jillian.baker@nottingham.ac.uk](mailto:jillian.baker@nottingham.ac.uk) (J.G.B.), [peter.kolb@uni-marburg.de](mailto:peter.kolb@uni-marburg.de) (P.K.)

**Running title:**  $\beta$ 1-selectivity of xamoterol and nebivolol

Jillian G Baker

Cell Signalling,

School of Life Sciences,

C Floor Medical School,

Queen's Medical Centre,

University of Nottingham,

Nottingham,

NG7 2UH,

UK.

Tel: +44 115 8230085

Fax: +44 115 8230081

[Jillian.baker@nottingham.ac.uk](mailto:Jillian.baker@nottingham.ac.uk)

Peter Kolb

Institute of Pharmaceutical Chemistry

Philipps-University Marburg

Marbacher Weg 6

35032 Marburg

Germany

Tel: +49 6421 28 25908

[peter.kolb@uni-marburg.de](mailto:peter.kolb@uni-marburg.de)

Text pages: 43

Tables: 4

Figures: 5

References: 34

Abstract: 240 words

Introduction: 701 words

Discussion: 1585 words

## **Abbreviations**

CHO: Chinese hamster ovary

EL: extracellular loop

PBS: phosphate buffered saline

sfm: serum free media

TM: transmembrane

WT: wildtype

MD: Molecular Dynamics

## Abstract

Known off-target interactions frequently cause predictable drug side-effects, e.g.  $\beta$ 1-antagonists (used for heart disease) risk  $\beta$ 2-mediated bronchospasm. Computer-aided drug design would improve if the structural basis of existing drug selectivity was understood. A mutagenesis approach determined the ligand-amino acid interactions required for  $\beta$ 1-selective affinity of xamoterol and nebivolol, followed by computer-based modelling to provide possible structural explanations.  $^3\text{H}$ -CGP12177 whole cell binding was conducted in CHO cells stably expressing human  $\beta$ 1,  $\beta$ 2 and chimeric  $\beta$ 1/ $\beta$ 2-adrenoceptors (ARs). Single point mutations were investigated in transiently transfected cells. Modelling studies involved docking ligands into three-dimensional receptor structures and performing Molecular Dynamics simulations, comparing interaction frequencies between *apo* and *holo* structures of  $\beta$ 1 and  $\beta$ 2-ARs. From these observations, an ICI89406 derivative was investigated that gave further insights into selectivity. Stable cell line studies determined that transmembrane 2 was crucial for the  $\beta$ 1-selective affinity of xamoterol and nebivolol. Single point mutations determined that the  $\beta$ 1-AR isoleucine (I118) rather than the  $\beta$ 2 histidine (H93) explained selectivity. Studies of other  $\beta$ 1-ligands found I118 was important for ICI89406 selective affinity but not that for betaxolol, bisoprolol or esmolol. Modelling studies suggested that the interaction energies and solvation of  $\beta$ 1-I118 and  $\beta$ 2-H93 are factors determining selectivity of xamoterol and ICI89406. ICI89406 without its phenyl group loses its high  $\beta$ 1-AR affinity, resulting in the same affinity as for the  $\beta$ 2-AR. The human  $\beta$ 1-AR residue I118 is crucial for the  $\beta$ 1-selective affinity of xamoterol, nebivolol and ICI89406, but not all  $\beta$ 1-selective compounds.

## **Significance statement – 79 words**

Some ligands have selective binding affinity for the human  $\beta_1$  versus the  $\beta_2$ -adrenoceptor however the molecular / structural reason for this is not known. The transmembrane 2 residue isoleucine I118 is responsible for the selective  $\beta_1$ -binding of xamoterol, nebivolol and ICI89406, but does not explain the selective  $\beta_1$ -binding of betaxolol, bisoprolol or esmolol. Understanding the structural basis of selectivity is important to improve computer aided ligand design and targeting I118 in  $\beta_1$ -adrenoceptors is likely to increase  $\beta_1$ -selectivity of drugs.

## Introduction.

Predictable side-effects from known off-target interactions frequently cause adverse drug effects. Thus, drug discovery efforts are increasingly centred around creating compounds that are highly selective for only the clinical target, in the expectation of maximising clinical effectiveness whilst minimising harm (Clarke and Bond, 1998). However, the precise structural basis of selectivity for most ligands and most GPCRs is poorly understood, including the long studied prototypical  $\beta$ -adrenoceptors ( $\beta$ -AR).

A clinical example of where receptor selectivity matters, and indeed careful control of all pharmacological characteristics is required for minimum harm, are  $\beta$ -blockers for cardiovascular disease.  $\beta$ -blockers are important in the management of heart failure and ischaemic heart disease, where blockade of the cardiac  $\beta_1$ -AR is thought to be the main therapeutic factor (Cruickshank, 2007). In those with heart failure,  $\beta$ -blockers lower mortality by ~35% and several different compounds have been shown to be beneficial (metoprolol, MERIT-HF, 1999; bisoprolol, CIBIS-II, 1999; carvedilol, COPERNICUS, Packer et al., 2002; nebivolol, SENIORS, Flather et al., 2005). A similar reduction in mortality is seen in ischaemic heart disease with a wider range of  $\beta$ -blockers (Baker and Wilcox 2017 and references therein). However, receptor selectivity is a concern: drugs with concomitant  $\beta_2$ -AR antagonism can cause bronchospasm in those with asthma and impair the efficacy of  $\beta_2$ -agonist rescue medication (Baker and Wilcox, 2017 and references therein). Therefore, such drugs remain contraindicated and, as a consequence, potentially life-saving treatment is denied to those with both asthma and heart disease. In the clinical scenario, efficacy, as well as affinity, matters. Xamoterol is a  $\beta_1$ -AR ligand which has a similar degree of  $\beta_1$ -selective affinity as nebivolol, but xamoterol also has partial agonist activity and its use was associated

with increased mortality (Xamoterol in Severe Heart Failure Study Group, 1990). Thus, controlling receptor selectivity and efficacy are clinically important.

Selective molecules are traditionally developed by an iterative medicinal chemistry-pharmacology process from a starting ligand, making small changes to the molecular structure, examining the pharmacological effects, and then synthesising further analogues, until the required characteristics have sufficiently been optimised. This basic medicinal chemistry technique was used in the original design of  $\beta$ -blockers (Black et al., 1965) and is still used to develop novel  $\beta$ -selective molecules (Baker et al., 2017), but it is costly both in terms of time and materials when done in a “trial and error” fashion. Given the recent advances in protein structure determination techniques, computer-aided ligand design approaches offer a real opportunity to reduce both the time and expense of novel drug development. Although there have been some areas where crystal structures have suggested a structural basis for subtype selectivity (e.g. angiotensin receptors Zhang et al., 2017; melatonin receptors Stauch et al., 2019), for many target proteins, there are either too few crystal structures with ligands of different selectivities, or these structures do not offer straightforward explanations for ligand selectivity between receptor subtypes. Thus, the structural basis for ligand selectivity, even for the prototypical  $\beta$ -AR, remains largely unknown (e.g.  $\beta$ 2-selectivity for ICI118551, structure PDB 3NY8). This makes rational drug design challenging.

There are however a few compounds where the structural basis for selectivity has been wholly or partly deciphered. Mutagenesis (including chimeric mutagenesis) approaches have uncovered suggestions for certain necessary ligand-amino acid interactions (e.g. Frielle et al., 1988; Marullo et al., 1990; Isogaya et al., 1999). From our previous work, the precise amino

acid interactions required for the highly  $\beta$ 2-selective affinity of salmeterol determined from chimeric mutagenesis studies (Baker et al., 2015) have been confirmed in the  $\beta$ 2-salmeterol crystal structure (Masureel et al., 2018).

This was an exploratory study with the aim of discovering the precise ligand-amino acid interactions that are important for the  $\beta$ 1- vs  $\beta$ 2-selectivity of two moderately selective  $\beta$ 1-AR ligands, xamoterol and nebivolol. We used a chimeric receptor mutagenesis approach, beginning with the whole receptor, then narrowing down to identify the amino acid(s) important for the selective affinity of these two ligands. This was followed by computational structure-based techniques to explain the molecular basis for the selective affinity of these ligands for the human  $\beta$ 1-AR over the  $\beta$ 2-AR. Having identified the important amino acids, studies were widened to determine whether this single amino acid could explain the selective affinity of other moderately selective compounds (ICI89406, bisoprolol, betaxolol and esmolol).



## Materials and Methods

### *Materials*

Molecular biology reagents were from Promega (Madison, WI, USA). Lipofectamine, pcDNA3.1, Top 10F competent cells and OPTIMEM were from Life Technologies (Paisley, UK). QuikChange mutagenesis kits were from Stratagene (La Jolla, CA) and foetal calf serum was from PAA Laboratories (Teddington, Middlesex, UK). <sup>3</sup>H-CGP12177 was from Amersham International (Buckinghamshire, UK) and Microscint 20 and Ultima Gold XR scintillation fluid from PerkinElmer (Shelton, CT, USA). Xamoterol (0950), ICI89406 (0832), and betaxolol (0906) were from Tocris Life Sciences (Avonmouth, UK). Nebivolol (SRP035255n) was from Sequoia (Pangbourne, UK). Bisoprolol (B2185) and esmolol (E8031) and all other reagents were from Sigma Aldrich (Poole, Dorset, UK). A derivative of ICI89406 without the terminal phenyl moiety (ICI89406np) was from MolPort (MolPort-031-323-389). The chemical structure of the drugs studied are shown of Figure 1.

### *Molecular biology*

The wildtype human  $\beta$ 1-adrenoceptor ( $\beta$ 1-WT), wild type human  $\beta$ 2-adrenoceptor ( $\beta$ 2-WT) and all transmembrane and extracellular region chimera constructs, as well as all stable cell lines, are as reported in Baker et al., 2014 and 2015. The single point mutations used here in (Tables 1 and 2) were generated using QuikChange mutagenesis and BioLine PolyMate Additive for GC-rich templates (as in Baker et al., 2014). After subcloning in Top 10F competent cells, each mutant cDNA was excised with Hind III/XbaI and subcloned into native pcDNA3.1 containing a neomycin selection marker. All mutations and sequences were confirmed by DNA sequencing using the School of Life Sciences Sequencing Facility.

### ***Cell culture***

CHO-K1 cells (RIDD: CVCL\_0214) stably transfected with the wildtype human  $\beta 1$  or  $\beta 2$ -adrenoceptor, or one of the full EL region or TM domain chimeric receptors (total 24 cell lines) were used (see Baker et al., 2014 and 2015 for full details). For transiently transfected cells the parent CHO-K1 cells were transfected in a T75 with 10 ng DNA in 100  $\mu$ l Lipofectamine and 8ml OPTIMEM as per manufacturer's instructions on day 1, the transfection reagents removed and replaced with media on day 2, the cells plated into 96-well plates on day 3 and the experiments performed on day 4. All CHO cells were grown in Dulbecco's modified Eagle's medium nutrient mix F12 (DMEM/F12), containing 10% foetal calf serum and 2 mM L-glutamine in a 37°C humidified 5% CO<sub>2</sub> : 95% air atmosphere. Cells were always grown in the absence of any antibiotics. Mycoplasma contamination is intermittently monitored within the laboratory (negative) but cell lines were not tested routinely with each experiment.

### ***<sup>3</sup>H-CGP12177 Whole Cell Binding***

Cells were grown to confluence in tissue-culture-treated white-sided 96-well view plates. The affinity ( $K_D$ , concentration required to bind half of the receptors) of <sup>3</sup>H-CGP12177 was determined for each construct from saturation binding experiments. The affinity for competing ligands was determined by incubating the competing ligand in the presence of a fixed concentration of <sup>3</sup>H-CGP12177, and as determined from inhibition of radioligand, is thus referred to as  $K_i$  values.

Briefly, the affinity ( $K_D$ ) of <sup>3</sup>H-CGP12177 was determined for each construct from saturation experiments, with concentrations of <sup>3</sup>H-CGP12177 in the range of 0.005 to 42.8 nM) and the  $K_i$  for competing ligands by incubating the competing ligand in the presence of a fixed

concentration of  $^3\text{H}$ -CGP12177 as previously described (Baker, 2005) in 200  $\mu\text{l}$  total well volume for 2 hrs at  $37^\circ\text{C}$  before being washed with 2 x 200 ml cold ( $4^\circ\text{C}$ ) PBS. A volume of 100  $\mu\text{l}$  Microscint 20 was then added to each well, the plates left for several hours before being counted on a Topcount for 2 min per well. Propranolol (10  $\mu\text{M}$ ) was used to define non-specific binding in all experiments.

### ***Data and statistical analysis***

#### *Whole cell binding*

The affinity of  $^3\text{H}$ -CGP12177 for each mutant was determined from saturation binding, using 10  $\mu\text{M}$  propranolol to determine non-specific binding and all data points were performed in quadruplicate. Specific binding (SB, equation 1) of  $^3\text{H}$ -CGP12177 at different concentrations of  $^3\text{H}$ -CGP12177 was fitted using the non-linear regression program Prism 7 to the equation:

$$\text{Equation 1: } \text{SB} = \frac{\text{A} \times \text{Bmax}}{\text{A} + \text{K}_\text{D}}$$

where A is the concentration of  $^3\text{H}$ -CGP12177, Bmax is the maximal specific binding and  $\text{K}_\text{D}$  is the dissociation constant of  $^3\text{H}$ -CGP12177.

The affinity of the other ligands was determined from competition binding. All data points were recorded in triplicate and each 96-well plate contained 6 determinations of total and non-specific binding. A sigmoidal concentration-response curve was then fitted to the data using Graphpad Prism 7 and the  $\text{IC}_{50}$  was determined as the concentration required to inhibit 50% of the specific binding using equation 2.

$$\text{Equation 2: } \% \text{ uninhibited binding} = 100 - \frac{(100 \times A)}{(A + IC_{50})} + NS$$

where A is the concentration of the competing ligand,  $IC_{50}$  is the concentration at which half of the specific binding of  $^3H$ -CGP12177 has been inhibited, and NS is the non-specific binding.

From the  $IC_{50}$  value and the known concentration of  $^3H$ -CGP12177, a  $K_i$  value (concentration at which half the receptors are bound by the competing ligand) was calculated using equation 3:

$$\text{Equation 3: } K_i = \frac{IC_{50}}{1 + ([^3H\text{-CGP12177}]/K_D \text{ } ^3H\text{-CGP12177})}$$

In order to explore whether a single receptor region (Table 1), or individual amino acid (Table 2) was statistically different from all of the others, a one-way ANOVA with post hoc Tukey analysis was conducted. The one-way ANOVA determines if there is a difference within the datasets as a whole, when comparing each mutant with each other and wildtype (e.g. xamoterol affinity at  $\beta 1$ -WT,  $\beta 1$ -TM1,  $\beta 1$ -TM2,  $\beta 1$ -TM3,  $\beta 1$ -TM4,  $\beta 1$ -TM5,  $\beta 1$ -TM6,  $\beta 1$ -TM7,  $\beta 1$ -N,  $\beta 1$ -EL1,  $\beta 1$ -EL2 and  $\beta 1$ -EL3 ) in a single statistical test. If the ANOVA does detect a difference, the post hoc analysis determines within the entire dataset which mutants have caused a change that is statistically different from wildtype, i.e. from  $\beta 1$ -WT. Thus, for the affinity of xamoterol, the one-way ANOVA determined that there was a significant difference between the datasets in the different mutants, and post hoc Tukey analysis that  $\beta 1$ -TM2 was different from  $\beta 1$ -WT with a p value of  $p < 0.000001$ .

### ***Modelling of Human $\beta$ 1-AR Structures.***

Active and inactive conformation structures of human  $\beta$ 1-AR were modelled using MODELLER (Webb and Sali, 2014). The inactive state was modelled based upon the template with PDB ID 2VT4 and the active state based on the template with PDB ID 3SN6. The G<sub>oss</sub> subunit was added to the  $\beta$ 1-AR active-state-model by superimposing this model with the ternary complex of the  $\beta$ 2-AR (PDB ID 3SN6) and removing the receptor portion and small-molecule ligand of 3SN6.

### ***$\beta$ 2-AR Crystal Structures.***

Crystal structures of the  $\beta$ 2-AR in an active or inactive conformation were obtained from the PDB, PDB IDs 3SN6 and 2RH1, respectively.

Given the partial agonist nature of xamoterol and ICI89406 (Mistry et al., 2013), both ligands were manually docked into both the active and inactive conformations of the receptors.

Betaxolol, bisoprolol and esmolol were docked into the inactive  $\beta$ 1- and  $\beta$ 2-AR structures only. Nebivolol was not docked or simulated due to the high number of chiral centres (4), which makes it impossible to determine the correct pose of each enantiomer and correlate the simulation results with the experimental evidence obtained for the racemate. Calculations were performed using Chemical Computing Group's Molecular Operating Environment 2019 (MOE; Chemical Computing Group ULC 1010 Sherbooke St. West Suite 910, Montreal QC, 2018).

### ***Molecular Dynamics Simulations.***

Molecular dynamics (MD) simulations of the  $\beta$ 1- and  $\beta$ 2-AR to investigate the structural basis of selectivity of the ligands tested were carried out in the NPT ensemble. Structures

were embedded in a homogeneous POPC bi-layer membrane with CHARMM-GUI's Membrane Builder (Lee, Patel et al., 2018) and solvated with TIP3P water in a 0.15 nM NaCl solution. The CHARMM36 force field and the CHARMM General Force Field (CGenFF) were used in the simulations. The prepared structures were first equilibrated with NAMD (Phillips et al., 2020), using parameters provided by CHARMM-GUI, at 300 K. Following equilibration, ACEMD3 (Harvey et al., 2009) was used for production runs. Five replicate calculations of 500 ns were performed for each system (with detailed values calculated from all replicates provided in Supp. Tables 1-4).

*Apo* (unbound) structures of both receptors and their states were simulated and used as control for the simulations of the *holo* (ligand-bound) proteins. Xamoterol and ICI89406 were simulated in complex with both active and inactive protein states because of their partial agonistic effect.

Interaction energy, hydrogen bond, solvation and water bridge analyses of the trajectories were performed using CPPTRAJ (Roe et al., 2013). The interaction energy is calculated as the sum of the van-der-Waals (Lennard-Jones potential) and electrostatic (Coulombic potential) terms individually for each frame and averaged over all frames. A hydrogen bond is defined to occur whenever a positively polarised hydrogen bound to a heteroatom is within 3 Å and at an angle of 135° to a heteroatom with a lone electron pair. An atom is defined to be solvated whenever it forms at least one hydrogen bond with a water molecule. Finally, a water bridge connects two groups, where each is able to form hydrogen bonds, via a water molecule. The three latter descriptors are calculated as the percentage of frames in a trajectory in which the respective feature occurs. *Holo* simulations were compared to the *apo* simulations for differences in hydrogen bonding, solvation, and water bridge formation.

Where appropriate, unpaired t-tests were performed, comparing the calculated values for all descriptors between unbound (*apo*) and bound (*holo*) structures, and between ICI89406 and ICI89406np in the different receptor structures and conformations.

### ***Sourcing analogue compounds***

Following the docking calculations and MD simulations, and based on the observed ligand:receptor interactions in these calculations, analogues of the initially investigated ligands were searched in the small-molecule database ZINC (Sterling & Irwin, 2015), using a similarity threshold of at least 30%. We were specifically looking for compounds that would miss key interaction motifs in regions highlighted as important by the pharmacological experiments. Thus, we wished to test the hypotheses generated based on the MD simulation data. No commercially available xamoterol analogues that fulfilled all the criteria were identified, but we identified and sourced ICI89406np (ICI89406 without the terminal phenyl group), and evaluated it pharmacologically.

## Results

### *Identification of the regions in the human $\beta$ 1-AR important for xamoterol and nebivolol affinity - stable cell lines.*

Xamoterol and nebivolol inhibited the specific binding of  $^3\text{H}$ -CGP12177 in CHO- $\beta$ 1-WT cells to yield log  $K_i$  values of -7.19 and -8.33 respectively (Table 1). In the  $\beta$ 2-WT cells the log  $K_i$  values were -5.89 and -6.93, giving a  $\beta$ 1 vs  $\beta$ 2 selectivity for these compounds of 20 and 25-fold for xamoterol and nebivolol respectively, in keeping with previous studies (Baker 2005, 2010).

When the affinity of these compounds was studied in cell lines expressing chimeric  $\beta$ 1-receptors, the affinity of xamoterol and nebivolol were reduced in the  $\beta$ 1-TM2 receptor (i.e. the  $\beta$ 1-AR but with mutations such that transmembrane helix 2 [TM2] is that of the  $\beta$ 2-AR) compared with all other  $\beta$ 1 receptors (WT and each single-region chimeric receptor; Table 1, Figure 2). This reduction in affinity, more closely resembling that of the affinity at the  $\beta$ 2-AR, suggests that this region contained one or more amino acids which form an important (direct or indirect) interaction with the ligands and therefore has a large impact on the binding selectivity of xamoterol and nebivolol. When the reciprocal receptors were studied (i.e.  $\beta$ 2-chimeric receptors), the affinity of xamoterol and nebivolol was significantly increased in the CHO- $\beta$ 2-TM2 cells, compared to  $\beta$ 2-WT and all other  $\beta$ 2-chimeras, again suggesting that this region is important for the selectivity of these two ligands (Table 1, Figure 2).

### *Identification of the individual amino acids involved in TM2 for xamoterol and nebivolol - transiently transfected cells.*

From the stable cell line experiments above, TM2 appeared to be the most important region for the selectivity of xamoterol and nebivolol. Single point mutations were therefore made at



each of the 7 sites in TM2 where amino acids between the two receptors are different. For example, at position 98 in the  $\beta$ 1-AR, a single point mutation was made such that this amino acid was mutated from a methionine M to a threonine T (i.e.  $\beta$ 1-M98T, Table 2). The reciprocal  $\beta$ 2 construct (e.g.  $\beta$ 2-AR with a single point mutation to the amino acid of the  $\beta$ 1-AR, e.g.  $\beta$ 2-T73M) was also made. Binding studies with the individual amino acid mutations revealed that of the  $\beta$ 1-TM2 constructs,  $\beta$ 1-I118H reduced the affinity of both xamoterol and nebivolol compared with  $\beta$ 1-WT (Table 2, Figure 3). When the reciprocal  $\beta$ 2-TM2 individual amino acid constructs were examined, the corresponding construct ( $\beta$ 2-H93I) had higher affinity for xamoterol and nebivolol (Table 2, Figure 3). Taken together, this suggests that this amino acid at position 118/93 is very important in determining the selective binding affinity of xamoterol and nebivolol.

***Determination of whether  $\beta$ 1-M98 can explain the  $\beta$ 1-selectivity of other  $\beta$ 1-antagonists – transiently transfected cells.***

Other  $\beta$ -ligands with moderate  $\beta$ 1-selectivity were then examined. ICI89406 (another  $\beta$ 1-partial agonist, Mistry et al., 2013), and betaxolol, bisoprolol and esmolol ( $\beta$ -antagonists without efficacy in these cells; Baker et al., 2011; Baker et al., 2017; Baker et al., 2020; Mistry et al., 2013) had  $\beta$ 1-WT (vs  $\beta$ 2-WT) binding affinity selectivities of 81-, 14-, 30- and 13-fold, respectively (Table 2, Figure 3). When ICI89406 was examined in the TM2 constructs, it also had reduced affinity in the  $\beta$ 1-I118H, compared to  $\beta$ 1-WT. An increase in affinity at the reciprocal  $\beta$ 2-H93I construct was also seen (compared with  $\beta$ 2-WT). The affinities of betaxolol and esmolol were unchanged in any of the TM2 constructs, whereas the affinity of bisoprolol was reduced by 2-fold by the  $\beta$ 1-I118H construct (which is of uncertain pharmacological significance).

### ***In silico ligand:receptor interaction analyses***

In order to understand the role of the isoleucine at position 118 in the  $\beta_1$ , compounds were docked into models and X-ray structures of the human  $\beta_1$  and  $\beta_2$ , respectively, and molecular dynamics simulations of these complexes were analysed. All docked and simulated compounds have one chiral centre and are the (*S*)-enantiomer at the common hydroxy group. Computed interaction energies, as well as hydrogen bond, solvation, and water-bridge formation frequencies were determined along the simulation trajectories (Tables 3 and 4) and were compared with the values obtained for the *apo* structures. Given the partial agonist nature of xamoterol and ICI89406, both compounds were examined in both the active and inactive structures of the human  $\beta_1$  and  $\beta_2$ , whilst the other 3 compounds (known antagonists) were examined in the inactive structures only.

### **Xamoterol**

In our simulations, xamoterol showed similar trends of solvation and interaction energies in both active and inactive  $\beta_1/\beta_2$ -ARs. In the  $\beta_2$  simulations, xamoterol reduced the solvation of H93's  $\epsilon$  nitrogen compared to the *apo* simulation (34.8% in *apo* vs. 18.9% in the bound form for the active conformation, 41.2% in *apo* vs. 24.4% in the bound form for the inactive conformation; Tables 3 and 4). However, calculated mean interaction energies showed that xamoterol interacts less favourably with I118 in  $\beta_1$ -AR than with H93 in  $\beta_2$  ( $-0.4 \pm 0.1$  kcal/mol and  $-2.8 \pm 0.2$  kcal/mol, respectively, in the active state,  $-0.7 \pm 0.1$  kcal/mol and  $-2.9 \pm 0.3$  kcal/mol, respectively, in the inactive state; Tables 3 and 4).

### **ICI89406**

ICI89406 affects H93 differently in active and inactive  $\beta_2$  MD simulations. In the active state, ICI89406 has more favourable interaction energies with I118 in the  $\beta_1$  ( $-2.5 \pm 0.2$

kcal/mol) compared to H93 in the  $\beta 2$  ( $-0.9 \pm 0.1$  kcal/mol). However, the difference in interaction energies for the inactive state between  $\beta 1/\beta 2$  was much smaller and not significant ( $-2.1 \pm 0.3$  kcal/mol and  $-1.9 \pm 0.7$  kcal/mol respectively). In the inactive  $\beta 2$ , ICI89406 hinders the solvation of H93's  $\epsilon$  nitrogen (41.2% in apo vs. 11.0% bound; Table 4) and disrupts the water bridge between H93 and D192 (20.3% in apo vs 2.1% bound; Table 4). However, this was not observed in the active state simulations of  $\beta 2$ .

### **Analogue ICI89406np**

No commercially available xamoterol analogues lacking key interaction motifs were found in ZINC. The derivative of ICI89406 lacking the terminal phenyl moiety (here termed ICI89406 no phenyl, abbreviated as ICI89406np) was docked and investigated further, as it seemed likely to be informative with respect to the investigation of the role of the isoleucine vs. histidine at the far end of the binding site. MD simulations showed that ICI89406np improved the solvation of the  $\epsilon$  nitrogen of H93 (11.0% for ICI89406 vs. 27.9% for ICI89406np; Table 3; Figure 4) and the water-bridge between H93 and D192 (2.1% for ICI89406 vs. 21.4% for ICI89406np; Table 4) compared to ICI89406 in the inactive conformation of the  $\beta 2$ . The same is not observed for active  $\beta 2$ . The interaction energies to I118 and H93 for ICI89406np were comparable for both active ( $-0.4 \pm 0.1$  kcal/mol to I118  $\beta 1$ ,  $-0.1 \pm 0.2$  kcal/mol to H93  $\beta 2$ ) and inactive state ( $-0.5 \pm 0.1$  kcal/mol to I118  $\beta 1$ ,  $-0.0 \pm 0.0$  kcal/mol to H93  $\beta 2$ ) simulations.

The experimental affinity of ICI89406np was then examined in the stable CHO- $\beta 1$ -WT and CHO- $\beta 2$ -WT cell lines. Whilst ICI89406 was 170-fold  $\beta 1$ -selective ( $\log K_i$  of  $-9.09 \pm 0.07$  and  $-6.86 \pm 0.06$ ,  $n=6$  for  $\beta 1$  and  $\beta 2$  respectively, in keeping with previous studies (Mistry et al., 2013), ICI89406np had far lower affinity for the  $\beta 1$ -WT, whilst that at the  $\beta 2$ -AR was

unchanged ( $\log K_i$   $-6.97 \pm 0.06$  and  $-7.04 \pm 0.05$ ,  $n=7$  for  $\beta_1$  and  $\beta_2$  respectively; Figure 5).

Thus, all  $\beta_1$  selectivity was lost with removal of the phenyl group.

### **Betaxolol, bisoprolol and esmolol**

Betaxolol, bisoprolol and esmolol were also examined in the inactive  $\beta_1$  and  $\beta_2$  structures and the effects on H93/I118 were small or statistically insignificant (Supp. Fig 2, and Supp Tables 3 and 4 for docking poses and nitrogen solvation, water-bridge formation and interaction energies). The only exception was for esmolol in  $\beta_2$ , where there was a significant improvement in the frequency of a water-bridge between H93 and D192 in  $\beta_2$ -AR (20.3% in apo vs 31.0% bound).

## Discussion

Computer-aided drug design offers a method for speeding up the drug discovery process, but to be accurate requires very high-quality computer models, which in turn require large volumes of high-quality data, be that pharmacological, or structural, or better – both. A good start is to understand the structural basis of current drug selectivity, beginning with the pharmacologically most simple parameter, affinity. To understand the structural reasons for receptor subtype selectivity, crystal structures of each ligand-receptor subtype are required, a process which is difficult, time consuming and costly, and often involves heavily mutated receptors (truncated and stabilised with additions or multiple mutations to reduce flexibility; Cherezov et al., 2007; Rasmussen et al., 2007; Warne et al., 2008). Even then, the structural data obtained may not offer sufficient information to understand ligand selectivity (e.g. structure PDB ID 3NY8 with the  $\beta$ 2-selective antagonist IC1118551), as X-ray structures are, by definition, static snapshots.

Other methods to understand selectivity use pharmacological techniques. These have the advantage of acquiring data from native (non-tagged, not stabilised) receptors expressed in living mammalian cells. The pharmacological outcome of single amino acid changes can be examined with far greater throughput than could be achieved with crystal structures.

Importantly,  $\beta$ -AR pharmacological methods and crystal structures have been in agreement, highlighting the same important ligand-amino acid interactions (salmeterol, Baker et al., 2015; Masureel et al., 2018). Finally, although pharmacological techniques are able to determine the sites of interaction and selectivity, they do not give the structural explanation. When this is combined with detailed receptor modelling studies, however, firstly explanations for the observed selectivity can be suggested, but secondly the existence of the pharmacological data increases the quality of the computer models, thus improving accuracy

of future predictions for novel drugs. At their most powerful, such investigations will make predictions, which can then be tested pharmacologically, thereby providing more than just *post hoc* hypotheses.

This study used a chimeric mutagenesis approach to understand the  $\beta_1$ - over  $\beta_2$ -selectivity for xamoterol and nebivolol. Initially, the TM2 region was found to be crucial, with single amino acid mutations highlighting that when the  $\beta_1$  amino acid I118 was mutated to an H (as in the  $\beta_2$ ), the affinity of xamoterol and nebivolol was reduced to within 2-fold of that of the  $\beta_2$ . Equally importantly, when the reciprocal receptors were studied, ( $\beta_2$ -AR where the equivalent amino acid was mutated from an H to an I at position 93), a gain in affinity was seen (in both TM2 region receptor and single point mutation) such that the affinity of xamoterol and nebivolol for  $\beta_2$ -H93I was within 2-fold of that for the  $\beta_1$ . This independently highlighted this amino acid's important role in the selectivity of these compounds.

To determine whether this single amino acid is important for all  $\beta_1$ -selective ligands, four other moderately selective  $\beta_1$ -ligands were examined. ICI89406 (a  $\beta_1$ -partial agonist Mistry et al., 2013) was found to be greatly affected by this mutation (reduced by 17-fold; Table 2).

MD simulations of xamoterol showed that in the  $\beta_2$ , xamoterol hinders the  $\epsilon$  nitrogen of H93 forming hydrogen bonds with water when compared to the *apo* (unbound) receptor (Tables 3 and 4; we note that many other properties investigated did not show significant differences) in both active and inactive states. This observation is consistent with selectivity, as *in silico* binding of xamoterol to  $\beta_2$  is less favourable because the ligand displaces water molecules that would otherwise interact with the  $\epsilon$  nitrogen of H93 in the *apo* receptor. The more favourable interaction with H93 in  $\beta_2$  ( $-2.8 \pm 0.2$  kcal/mol compared to  $-0.4 \pm 0.1$  kcal/mol in

$\beta$ 1-active state,  $-2.9 \pm 0.3$  kcal/mol compared to  $-0.7 \pm 0.1$  kcal/mol in  $\beta$ 1-inactive state) might not be sufficient to compensate for the difference arising from the solvation pattern. Solvation of the  $\delta$  nitrogen of H93 was not considered, as it is pointing away from the ligand.

For ICI89406, a possible explanation is not as straightforward across the different activation states. In the  $\beta$ 2-inactive, ICI89406 also disrupts the solvation (41.2% in apo vs. 11.0% bound) and water bridge formation (20.3% in apo vs. 2.1% bound) of H93 in  $\beta$ 2-AR compared to the *apo* structure. However, this is not observed in the  $\beta$ 2-active state. In the active state, ICI89406 displays more favourable interaction energies to  $\beta$ 1-I118 than  $\beta$ 2-H93 ( $-2.2 \pm 0.2$  kcal/mol to  $\beta$ 1-I118 vs.  $-0.9 \pm 0.1$  kcal/mol to  $\beta$ 2-H93). This is likely due to the non-polar terminal phenyl group ability to form more favourable hydrophobic interactions with the non-polar  $\beta$ 1-I118 than with the polar  $\beta$ 2-H93. This can be garnered from the different van der Waals interaction energies compared to  $\beta$ 2-inactive. The difference between the active and inactive state interactions for ICI89406 is likely due to the size and shape of the pocket. In  $\beta$ 2-active, ICI89406 adopts a different position (Supp. Fig. 1) that causes it to be further away from H93, resulting in lower van der Waals interaction energies compared to the inactive state ( $-0.9 \pm 0.1$  kcal/mol in  $\beta$ 2-active vs.  $-2.4 \pm 0.4$  kcal/mol in  $\beta$ 2-inactive). In contrast,  $\beta$ 2-active, ICI89406's phenyl group is closer to H93, thereby disrupting the solvation despite a more favourable overall interaction energy. Both the poses in the active and the inactive state support  $\beta$ 1-selectivity, albeit for different reasons, indicating that the mechanism behind selectivity for these ligands is not as simple as one might envision. By considering the different states of the protein, we were able to suggest a more complete picture of the potential molecular explanations behind selectivity.

When ICI89406np (ICI89406 lacking the terminal phenyl group), was examined experimentally in  $\beta$ 1-WT and  $\beta$ 2-WT receptors, the loss of the phenyl group had no effect on  $\beta$ 2-AR affinity. However, the  $\beta$ 1-WT affinity was dramatically reduced, to that of the  $\beta$ 2-WT. This suggests that ICI89406's selectivity can be partially attributed to the interaction of the phenyl group with I118/H93. MD simulations of ICI89406np suggest that without the phenyl group, it is not able to disrupt the solvation of H93's  $\epsilon$  nitrogen or the water-bridge between H93 and D192 in  $\beta$ 2 in both  $\beta$ 2-active and  $\beta$ 2-inactive states (Tables 2 and 3). The interaction energies to  $\beta$ 1-I118 and  $\beta$ 2-H93 are comparable in both states (Tables 2 and 3). The low interaction energies suggest that the phenyl group plays an important role interacting with I118 in  $\beta$ 1-AR and H93 in  $\beta$ 2. Given similar moieties on the right part of xamoterol (Figure 1), the morpholine group might play a similar role.

For the other three  $\beta$ 1-AR compounds, betaxolol, bisoprolol and esmolol (which are neutral antagonists in these cells; Baker et al., 2011; Baker et al., 2017; Baker et al., 2020; Mistry et al., 2013), their moderate  $\beta$ 1-selectivity was not affected at the  $\beta$ 1-I118H, nor the  $\beta$ 2-H93I receptor (nor indeed any other amino acid in TM2). While statistically significant, the result for bisoprolol (a reduction in affinity from  $\log K_i$  -7.96  $\beta$ 1-AR to -7.69 in  $\beta$ 2-I118H) corresponds to a less than 2-fold decrease in affinity so is of uncertain significance. The ligand-amino acid interactions that are important for these compounds' selectivity must therefore lie elsewhere. This is in keeping with Marullo et al., 1990 who already hinted that different ligands may involve different amino acid interactions.

Docking of betaxolol, bisoprolol and esmolol to  $\beta$ 1 and  $\beta$ 2-inactive structures showed a distinct similarity between the poses of all three compounds - the isopropyl group next to the  $\beta$ -hydroxylamine was positioned in a similar location (Supp. Fig. 2). The isopropyl group of



these compounds is a considerable distance away from I118 (6.3 Å between the closest atoms). Therefore, this group is unlikely to have any direct interaction with I118, nor can it interfere with solvation of this residue, and thus the mutation I118H does not affect these compounds. MD simulations also showed little to no difference in solvation and interaction energies to these residues (Table 4).

As xamoterol and ICI89406 are partial agonists at both the human  $\beta_1$  and  $\beta_2$ -adrenoceptor, their partial agonist nature is not dependent on whether a I or H is present in TM2 (Mistry et al., 2013). Nebivolol stimulates such a poor partial agonist response it is barely measurable despite a high receptor expression level in these cells (Baker 2010). Ligand-amino acid interaction elsewhere on the receptor must therefore be important for determining the efficacy of compounds, and this TM2 residue identified is only responsible for determining the  $\beta_1$ -selective affinity interaction of certain  $\beta_1$ -selective compounds.

In conclusion, the isoleucine at position 118 in TM2 of the human  $\beta_1$ -adrenoceptor is an important interaction site for explaining the  $\beta_1$  vs  $\beta_2$  selectivity affinity of xamoterol, nebivolol and ICI89406. The most likely structural explanation is based upon the computational observation that those moieties on the affected ligands close to I118 can interact and interfere with the solvation of this residue. This plays a more important role for the polar H of the  $\beta_2$ -AR, but is less influential with the apolar I. Importantly, however, this amino acid does not explain the selectivity of other  $\beta_1$ -selective ligands, such as betaxolol, bisoprolol and esmolol, despite similar  $\beta_1$ -selective affinities compared to xamoterol, nebivolol and ICI89406. Thus betaxolol, bisoprolol and esmolol must also be interacting with amino acids in different parts of the receptor in order to achieve their selectivity. Overall, it therefore appears that different ligands, even with similar pharmacological characteristics,

interact with different amino acids to achieve their pharmacological outcome. However, if novel  $\beta$ -compounds with  $\beta$ 1-affinity selectivity were to be designed, compounds designed to interact with I118 in TM2 may well have higher selectivity, and therefore less potential for causing bronchospasm, than those that do not.

## **Acknowledgements**

We thank June McCulloch for technical assistance with tissue culture and washing the binding experiments and Frank Balzer for system maintenance of the computer infrastructure used in the computational experiments.

## **Authorship contributions**

Participated in research design: Lim, Kolb, Baker

Conducted experiments: Lim, Proudman, Monteleone, Baker

Contributed new reagents or analytical tools: Proudman

Performed data analysis: Lim, Kolb, Baker

Wrote or contributed to the writing of the manuscript: Lim, Kolb, Baker

## **Datasharing / Availability of data**

Data will be available on request from the corresponding authors.

## References

Baker JG (2005). The selectivity of  $\beta$ -adrenoceptor antagonists at the human  $\beta_1$ ,  $\beta_2$  and  $\beta_3$  adrenoceptors. *Br. J. Pharmacol.* **144**: 317-322.

Baker JG (2010) The selectivity of  $\beta$ -adrenoceptor agonists at the human  $\beta_1$ ,  $\beta_2$  and  $\beta_3$  adrenoceptors. *Br. J. Pharmacol* **160**: 148-161.

Baker JG, Wilcox RG. (2017)  $\beta$ -Blockers, heart disease and COPD: current controversies and uncertainties. *Thorax.* **72**: 271-276.

Baker JG, Kemp P, March J, Fretwell L, Hill SJ, Gardiner SM. (2011) Predicting in vivo cardiovascular properties of  $\beta$ -blockers from cellular assays: a quantitative comparison of cellular and cardiovascular pharmacological responses. *FASEB J* **25**: 4486-4497.

Baker JG, Fromont C, Bruder M, Thompson KSJ, Kellam B, Hill SJ, Fischer PM (2020) Using esterase selectivity to determine the in vivo duration of systemic availability and abolish systemic side-effects of topical  $\beta$ -blockers. *ACS Pharmacol Transl Sci.* **3(4)**: 737-748. doi: 10.1021/acsptsci.0c00051.

Baker JG, Gardiner SM, Woolard J, Fromont C, Jadhav GP, Mistry SN, Thompson KSJ, Kellam B, Hill SJ, Fischer PM. (2017) Novel selective  $\beta_1$ -adrenoceptor antagonists for concomitant cardiovascular and respiratory disease. *FASEB J.* **31**: 3150-3166.

Baker JG, Proudman RGW, Hill SJ (2014) Identification of key residues in transmembrane 4 responsible for the secondary, low affinity conformation of the human  $\beta$ 1-adrenoceptor. *Mol Pharmacol.* **85**: 811-829.

Baker JG, Proudman RGW, Hill SJ (2015) Salmeterol's extreme  $\beta$ 2-selectivity is due to residues in both extracellular loops and transmembrane domains. *Mol Pharmacol.* **87**: 103-120.

Black JW, Duncan WA, Shanks RG. (1965) Comparison of some properties of pronethalol and propranolol. *Br J Pharmacol Chemother* **25**: 577-91.

Chemical Computing Group ULC 1010 Sherbooke St. West Suite 910, Montreal QC, C.H. 2R7 (2018). Molecular Operating Environment (MOE).

Cherezov V, Rosenbaum DM, Hanson MA, Rasmussen SG, Thian FS, Kobilka TS, Choi HJ, Kuhn P, Weis WI, Kobilka BK, Stevens RC. (2007) High-resolution crystal structure of an engineered human beta2-adrenergic G protein-coupled receptor. *Science.* **318**: 1258-65.

CIBIS-II Investigators and Committees: The Cardiac Insufficiency Bisoprolol Study II (CIBIS-II): a randomised trial. (1999) *Lancet* **353**: 9-13.

Clarke WP, Bond RA (1998). The elusive nature of intrinsic efficacy. *Trends Pharmacol. Sci.* **19**: 270-276.

Cruickshank JM (2007) Are we misunderstanding beta-blockers. *Int J Cardiol.* **120**: 10-27.

Flather MD, Shibata MC, Coats AJ, Van Veldhuisen DJ, Parkhomenko A, Borbola J, Cohen-Solal A, Dumitrascu D, Ferrari R, Lechat P, Soler-Soler J, Tavazzi L, Spinarova L, Toman J, Böhm M, Anker SD, Thompson SG, and Poole-Wilson PA (2005) SENIORS Investigators. Randomized trial to determine the effect of nebivolol on mortality and cardiovascular hospital admission in elderly patients with heart failure (SENIORS). *Eur. Heart. J.* **26**: 215-25.

Frielle T, Daniel KW, Caron MG, Lefkowitz RJ (1988) Structural basis of beta-adrenergic receptor subtype specificity studied with chimeric beta 1/beta 2-adrenergic receptors. *Proc Natl Acad Sci U S A.* **85**: 9494-9498.

Harvey MJ, Giupponi G, and Fabritiis G de (2009). ACEMD: Accelerating Biomolecular Dynamics in the Microsecond Time Scale. *Journal of Chemical Theory and Computation* **5**: 1632–1639.

Isogaya M, Sugimoto Y, Tanimura R, Tanaka R, Kikkawa H, Nagao T, Kurose H (1999) Binding pockets of the beta(1)- and beta(2)-adrenergic receptors for subtype-selective agonists. *Mol Pharmacol.* **56**: 875-885.

Lee J, Pate, DS, Stähle J, Park S-J, Kern NR, Kim S, et al. (2018). CHARMM-GUI Membrane Builder for Complex Biological Membrane Simulations with Glycolipids and Lipoglycans. *Journal of Chemical Theory and Computation* **15**: 775–786.

Marullo S, Emorine LJ, Strosberg AD, Delavier-Klutchko C. (1990) Selective binding of ligands to beta 1, beta 2 or chimeric beta 1/beta 2-adrenergic receptors involves multiple subsites. *EMBO J.* **9**: 1471-1476.

Masureel M, Zou Y, Picard LP, van der Westhuizen E, Mahoney JP, Rodrigues JPGLM, Mildorf TJ, Dror RO, Shaw DE, Bouvier M, Pardon E, Steyaert J, Sunahara RK, Weis WI, Zhang C, Kobilka BK. (2018) Structural insights into binding specificity, efficacy and bias of a  $\beta$ 2AR partial agonist. *Nat Chem Biol.* **14**: 1059-1066.

MERIT-HF Study Group: Effect of metoprolol CR/XL in chronic heart failure: Metoprolol CR/XL Randomised Intervention Trial in Congestive Heart Failure (MERIT-HF). (1999) *Lancet* **353**: 2001-2007.

Mistry SN, Baker JG, Fischer PM, Hill SJ, Gardiner SM, Kellam B (2013) The synthesis, in vitro and in vivo characterisation of highly  $\beta$ 1-selective  $\beta$ -adrenoceptor partial agonists. *J Med Chem* **56**: 3852-3865.

Packer M, Fowler MB, Roecker EB, Coats AJS, Katus HA, Krum H, Mohacsi P, Rouleau JL, Tendera M, Staiger C, Holcslaw TL, Amann-Zalan I, and DeMets DL, for the Carvedilol Prospective Randomized Cumulative Survival (COPERNICUS) Study Group. (2002) Effect of Carvedilol on the Morbidity of Patients With Severe Chronic Heart Failure: Results of the Carvedilol Prospective Randomized Cumulative Survival (COPERNICUS) Study. *Circulation.* **106**: 2194-2199.

Phillips JC, Hardy DJ, Maia JDC, Stone JE, Ribeiro J v, Bernardi RC, et al. (2020). Scalable molecular dynamics on CPU and GPU architectures with NAMD. *The Journal of Chemical Physics* **153**: 044130.

Rasmussen SG, Choi HJ, Rosenbaum DM, Kobilka TS, Thian FS, Edwards PC, Burghammer M, Ratnala VR, Sanishvili R, Fischetti RF, Schertler GF, Weis WI, Kobilka BK. (2007) Crystal structure of the human beta2 adrenergic G-protein-coupled receptor. *Nature*. **450**: 383-7.

Roe, DR, Thomas E, Cheatham, I. (2013). PTRAJ and CPPTRAJ: Software for Processing and Analysis of Molecular Dynamics Trajectory Data. *Journal of Chemical Theory and Computation* **9**: 3084–3095.

Soisson SM, Stevens RC, Katritch V, Cherezov V. (2017) Structural basis for selectivity and diversity in angiotensin II receptors. *Nature*. **544**: 327-332.

Stauch B, Johansson LC, McCorvy JD, Patel N, Han GW, Huang XP, Gati C, Batyuk A, Slocum ST, Ishchenko A, Brehm W, White TA, Michaelian N, Madsen C, Zhu L, Grant TD, Grandner JM, Shiriaeva A, Olsen RHJ, Tribo AR, Yous S, Stevens RC, Weierstall U, Katritch V, Roth BL, Liu W, Cherezov V. (2019) Structural basis of ligand recognition at the human MT1 melatonin receptor. *Nature*. **569**: 284-288.

Sterling T, Irwin JJ. (2015) ZINC 15 – Ligand Discovery for Everyone. *Journal of Chemical Information and Modeling*. **55**: 2324-2337.



Warne T, Serrano-Vega MJ, Baker JG, Moukhametzianov R, Edwards PC, Henderson R, Leslie AG, Tate CG, Schertler GF. (2008) Structure of a  $\beta$ 1-adrenergic G-protein coupled receptor. *Nature* **454**: 486-491

Webb B, and Sali, A. (2014). Comparative Protein Structure Modeling Using Modeller. *Current Protocols in Bioinformatics*, John Wiley & Sons, Inc., 5.6.1-5.6.32.

Xamoterol in severe heart failure. (1990) The Xamoterol in Severe Heart Failure Study Group. *Lancet* **336**: 1-6.

Zhang H, Han GW, Batyuk A, Ishchenko A, White KL, Patel N, Sadybekov A, Zamlynny B, Rudd MT, Hollenstein K, Tolstikova A, White TA, Hunter MS, Weierstall U, Liu W, Babaoglu K, Moore EL, Katz RD, Shipman JM, Garcia-Calvo M, Sharma S, Sheth P, Soisson SM, Stevens RC, Katritch V, Cherezov V (2017) Structural basis for selectivity and diversity in angiotensin II receptors. *Nature*. **544**: 327-332.

## **Funding**

This research was funded in whole, or in part, by the Wellcome Trust [Grant number 086039/Z/08/Z]. For the purpose of open access, the author has applied a CC BY public copyright license to any Author Accepted Manuscript version arising from this submission. P.K. thanks the German Research Foundation DFG for Heisenberg professorship grants KO4095/4-1 and KO4095/5-1.

## **Conflicts of interest**

JGB has been on the Scientific Advisory Board for CuraSen Therapeutics since 2019. Most of the pharmacology work presented here pre-dates that appointment.

## Figure legends

Figure 1.

Chemical structures of xamoterol, nebivolol, ICI89406, ICI89406np, betaxolol, bisoprolol and esmolol.

Figure 2

a) Xamoterol inhibition of  $^3\text{H}$ -CGP12177 binding in a) and b) CHO- $\beta$ 1-WT and CHO- $\beta$ 1-TM2 cells and c) and d) CHO- $\beta$ 2-WT and CHO- $\beta$ 2-TM2 cells by xamoterol (a and c) and nebivolol (b and d). Non-specific binding was determined by 10  $\mu\text{M}$  propranolol in all cases. These are raw data (dpm) from single experiments with data from 2 different cell lines plotted on the same graph. The concentration of  $^3\text{H}$ -CGP12177 present in these experiments was a) 0.73 nM, b) 0.43nM c) 0.89 nM. and d) 0.49 nM and are representative of a) 8, b) 6, c) 7 and d) 6 separate experiments. Data points are mean  $\pm$  SD of triplicate determinations. e) the sequence alignment of the amino acid residues in TM2 of the  $\beta$ 1-WT and  $\beta$ 2-WT receptor

Figure 3

Inhibition of  $^3\text{H}$ -CGP12177 whole cell binding by a) xamoterol, b) nebivolol, c) ICI89406, d) betaxolol, e) bisoprolol and f) esmolol in transiently transfected cells. As data from three different transiently transfected constructs are shown on each graph, for clarity data are normalised to that for total and non-specific (as determined from an average of 6 wells on each plate) within each transfection. Non-specific binding was determined by 10  $\mu\text{M}$  propranolol. The concentration of  $^3\text{H}$ -CGP12177 present in these experiments was a) 0.57 nM, b) 0.49 nM, c) 0.49 nM, d) 0.63 nM, e) 0.57 nM and f) 0.68 nM and is

representative of a) 7, b) 7, c) 6, d) 6, e) 6 and f) 5 separate experiments. Data points are mean  $\pm$  SD of triplicate determinations.

#### Figure 4

Docking pose of (a) xamoterol in active  $\beta$ 1-(Green) and  $\beta$ 2-AR (Blue), and (b) ICI89406 and (c) ICI89406np in inactive  $\beta$ 1-(Green) and  $\beta$ 2-AR (Blue).

#### Figure 5

Inhibition of  $^3\text{H}$ -CGP12177 whole cell binding by ICI89406 and ICI89406np in a) CHO- $\beta$ 1-WT and b) CHO- $\beta$ 2-WT cells. Non-specific binding was determined by 10  $\mu\text{M}$  propranolol. The concentration of  $^3\text{H}$ -CGP12177 present in these experiments was 0.75 nM and they are representative of 6 separate experiments in each case. Data points are mean  $\pm$  SD of triplicate determinations.

Table 1

Affinity (log  $K_i$  values) of  $\beta$ -adrenoceptor ligands for the  $\beta_1$ -WT and  $\beta_2$ -WT obtained from  $^3\text{H}$ -CGP12177 whole cell binding in cells stably transfected with whole TM or EL changes.

The values are mean  $\pm$  s.e.mean for n separate experiments. The  $\beta_1$  over  $\beta_2$ -selectivity for the wildtype receptors is also given, thus xamoterol had 20-fold higher affinity for  $\beta_1$  than  $\beta_2$ .

	Log $K_i$ xamoterol	n	Log $K_i$ nebivolol	n
$\beta_1$ -WT	-7.19 $\pm$ 0.04	25	-8.33 $\pm$ 0.05	14
$\beta_1$ -N	-7.10 $\pm$ 0.11	5	-8.18 $\pm$ 0.11	10
$\beta_1$ -EL1	-7.38 $\pm$ 0.08	5	-8.35 $\pm$ 0.07	10
$\beta_1$ -EL2	-7.01 $\pm$ 0.11	5	-8.11 $\pm$ 0.09	10
$\beta_1$ -EL3	-7.41 $\pm$ 0.13	5	-8.10 $\pm$ 0.09	10
$\beta_1$ -TM1	-7.31 $\pm$ 0.08	8	-8.53 $\pm$ 0.04	6
$\beta_1$ -TM2	-6.35 $\pm$ 0.05****	8	-7.32 $\pm$ 0.07****	6
$\beta_1$ -TM3	-7.17 $\pm$ 0.08	8	-8.15 $\pm$ 0.09	6
$\beta_1$ -TM4	-7.41 $\pm$ 0.08	8	-7.91 $\pm$ 0.09*	6
$\beta_1$ -TM5	-7.24 $\pm$ 0.08	8	-8.28 $\pm$ 0.05	6
$\beta_1$ -TM6	-6.97 $\pm$ 0.09	7	-7.93 $\pm$ 0.05*	6
$\beta_1$ -TM7	-6.89 $\pm$ 0.10	7	-8.06 $\pm$ 0.06	6
$\beta_2$ -WT	-5.89 $\pm$ 0.03	30	-6.93 $\pm$ 0.06	12
$\beta_2$ -N	-5.97 $\pm$ 0.11	8	-6.89 $\pm$ 0.08	10
$\beta_2$ -EL1	-5.85 $\pm$ 0.04	8	-7.05 $\pm$ 0.04	10
$\beta_2$ -EL2	-6.06 $\pm$ 0.05	8	-6.82 $\pm$ 0.05	9

$\beta$ 2-EL3	$-5.91 \pm 0.06$	8	$-7.15 \pm 0.07$	10
$\beta$ 2-TM1	$-5.85 \pm 0.04$	8	$-7.05 \pm 0.06$	6
$\beta$ 2-TM2	$-6.84 \pm 0.07^{****}$	7	$-7.74 \pm 0.12^{****}$	6
$\beta$ 2-TM3	$-6.01 \pm 0.07$	8	$-6.76 \pm 0.03$	6
$\beta$ 2-TM4	$-5.68 \pm 0.04$	7	$-6.90 \pm 0.03$	6
$\beta$ 2-TM5	$-5.89 \pm 0.03$	6	$-6.95 \pm 0.02$	6
$\beta$ 2-TM6	$-6.09 \pm 0.05$	7	$-6.91 \pm 0.05$	6
$\beta$ 2-TM7	$-6.23 \pm 0.04^{***}$	9	$-6.97 \pm 0.08$	6
$\beta$ 1-selectivity	20.0		25.1	

\*\*\*\* $p < 0.000001$  One-way ANOVA with post hoc Tukey comparing values from the mutant receptors with those obtained from the  $\beta$ 1-WT or the  $\beta$ 2-WT.

\*\*\* $p < 0.00003$  and \* $p < 0.05$  compared with  $\beta$ 1-WT or the  $\beta$ 2-WT

Table 2

Affinity (log  $K_i$  values) of  $\beta$ -adrenoceptor ligands for the  $\beta_1$ -WT,  $\beta_2$ -WT and receptors containing single point mutations in TM2 obtained from  $^3\text{H}$ -CGP12177 whole cell binding in transiently transfected populations of cells. The  $K_D$  values of  $^3\text{H}$ -CGP12177 and the receptor expression levels obtained from saturation studies in these transient populations are given. The values are mean  $\pm$  s.e.mean for n separate experiments. The  $\beta_1$  over  $\beta_2$ -selectivity for the wildtype receptors is also given.

	$K_D$ $^3\text{H}$ - CGP12177	fmol/mg protein		Log $K_i$ xamoterol	n	Log $K_i$ nebivolol	n	Log $K_i$ ICI89406	n	Log $K_i$ betaxolol	n	Log $K_i$ bisoprolol	n	Log $K_i$ esmolol	n
$\beta_1$ -WT	0.28 $\pm$ 0.02#	731 $\pm$ 96	27	-7.13 $\pm$ 0.04	12	-8.01 $\pm$ 0.09	11	-8.88 $\pm$ 0.07	7	-8.07 $\pm$ 0.06	6	-7.96 $\pm$ 0.05	11	-6.65 $\pm$ 0.08	7
$\beta_1$ -M98T	0.31 $\pm$ 0.03	620 $\pm$ 109	6	-7.30 $\pm$ 0.10	7	-7.85 $\pm$ 0.12	6	-9.01 $\pm$ 0.11	5	-8.10 $\pm$ 0.05	7	-8.01 $\pm$ 0.05	6	-6.69 $\pm$ 0.08	5
$\beta_1$ -S102C	0.25 $\pm$ 0.03	430 $\pm$ 68	6	-7.21 $\pm$ 0.07	7	-7.93 $\pm$ 0.12	7	-8.84 $\pm$ 0.06	7	-8.03 $\pm$ 0.05	7	-8.00 $\pm$ 0.05	7	-6.78 $\pm$ 0.04	5
$\beta_1$ -L110A	0.22 $\pm$ 0.02	334 $\pm$ 80	5	-7.31 $\pm$ 0.06	6	-7.94 $\pm$ 0.11	6	-8.93 $\pm$ 0.07	6	-8.22 $\pm$ 0.06	6	-8.12 $\pm$ 0.09	5	-6.74 $\pm$ 0.08	5
$\beta_1$ -T117A	0.26 $\pm$ 0.03	414 $\pm$ 61	6	-7.05 $\pm$ 0.08	6	-7.87 $\pm$ 0.10	8	-8.66 $\pm$ 0.04	6	-7.98 $\pm$ 0.08	6	-7.88 $\pm$ 0.07	6	-6.66 $\pm$ 0.03	5
$\beta_1$ -I118H	0.21 $\pm$ 0.03	292 $\pm$ 73	6	-6.33 $\pm$ 0.09***	8	-7.29 $\pm$ 0.09***	7	-7.64 $\pm$ 0.04***	6	-7.80 $\pm$ 0.04	8	-7.69 $\pm$ 0.04*	6	-6.33 $\pm$ 0.05	7
$\beta_1$ -V119I	0.30 $\pm$ 0.05	340 $\pm$ 76	6	-7.27 $\pm$ 0.06	8	-7.89 $\pm$ 0.10	7	-9.21 $\pm$ 0.06*	7	-8.07 $\pm$ 0.08	6	-7.95 $\pm$ 0.08	6	-6.65 $\pm$ 0.07	7
$\beta_1$ -V120L	0.28 $\pm$ 0.04	528 $\pm$ 129	6	-7.11 $\pm$ 0.08	6	-7.73 $\pm$ 0.09	7	-8.69 $\pm$ 0.07	7	-8.10 $\pm$ 0.10	6	-7.89 $\pm$ 0.05	5	-6.66 $\pm$ 0.15	6
$\beta_2$ -WT	0.18 $\pm$ 0.01#	165 $\pm$ 13	30	-5.96 $\pm$ 0.06	7	-6.88 $\pm$ 0.12	7	-6.97 $\pm$ 0.08	7	-6.92 $\pm$ 0.07	6	-6.49 $\pm$ 0.07	7	-5.53 $\pm$ 0.12	5
$\beta_2$ -T73M	0.22 $\pm$ 0.03	59 $\pm$ 11	10	-5.76 $\pm$ 0.05	8	-6.94 $\pm$ 0.12	8	-6.90 $\pm$ 0.06	8	-6.83 $\pm$ 0.08	8	-6.51 $\pm$ 0.13	8	-5.69 $\pm$ 0.09	7
$\beta_2$ -C77S	0.22 $\pm$ 0.03	18 $\pm$ 3	10	-5.89 $\pm$ 0.13	10	-6.97 $\pm$ 0.07	11	-6.79 $\pm$ 0.12	9	-6.94 $\pm$ 0.13	8	-6.28 $\pm$ 0.11	10	-5.42 $\pm$ 0.15	8

$\beta$ 2-A85L	0.22 ± 0.05	38 ± 6	13	-5.75 ± 0.05	10	-6.85 ± 0.10	10	-6.77 ± 0.09	10	-6.88 ± 0.08	11	-6.22 ± 0.05	11	-5.67 ± 0.11	11
$\beta$ 2-A92T	0.25 ± 0.04	48 ± 6	12	-5.63 ± 0.10	8	-6.86 ± 0.14	7	-6.71 ± 0.08	9	-6.84 ± 0.07	8	-6.36 ± 0.07	8	-5.34 ± 0.18	8
$\beta$ 2-H93I	0.30 ± 0.05	20 ± 2	12	-6.82 ± 0.07***	9	-7.76 ± 0.11***	9	-7.59 ± 0.14**	11	-7.07 ± 0.09	11	-6.51 ± 0.11	8	-5.87 ± 0.09	11
$\beta$ 2-I94V	0.21 ± 0.03	35 ± 5	11	-5.99 ± 0.08	12	-6.90 ± 0.08	12	-6.83 ± 0.09	12	-7.02 ± 0.08	12	-6.48 ± 0.10	12	-5.32 ± 0.10	12
$\beta$ 2-L95V	0.20 ± 0.03	38 ± 5	10	-6.29 ± 0.09	11	-7.17 ± 0.09	11	-6.94 ± 0.10	9	-7.11 ± 0.06	11	-6.42 ± 0.11	11	-5.54 ± 0.09	11
$\beta$ 1-selectivity				14.8		13.5		81.3		14.1		29.5		13.2	

#saturation data from Baker et al., 2015

\*\*\* $p < 0.0001$  One-way ANOVA with post hoc Tukey comparing values from the mutant receptors with those obtained from the  $\beta$ 1-WT or the  $\beta$ 2-WT.

\*\* $p < 0.003$  and \* $p < 0.05$  compared with  $\beta$ 1-WT or the  $\beta$ 2-WT

Table 3.

Table of interaction energies, solvation, and water-bridges of ligand and important residues calculated from MD simulations for ligands examined in the active structures. Numerical values are calculated as percentage of frames (for nitrogen solvation and water bridge formation) and the interaction energy is given in kcal/mol. Values are mean  $\pm$  sem of n separate determinations. Compounds are compared with values obtained in the unbound (*apo*) structure using an unpaired t-test. The difference in the interaction energy to I118/H93 is also given between the compound binding to the  $\beta$ 1-WT and  $\beta$ 2-WT and compared using an unpaired t-test. Full details of each replicate, and all p values are given in Supp. Table 1 and 2.

	Unbound <i>apo</i>	n	xamoterol	n	ICI89406	n	ICI89406np	n
$\beta$ 1-WT -active								
$\beta$ 1-I118 LIG electrostatic energy			0.8 $\pm$ 0.1	5	-0.0 $\pm$ 0.1	5	0.0 $\pm$ 0.1	5
$\beta$ 1-I118 LIG Van der Waals energy			-1.2 $\pm$ 0.1	5	-2.5 $\pm$ 0.2 <sup>†</sup>	5	-0.4 $\pm$ 0.0 <sup>†</sup>	5
$\beta$ 1-I118 LIG Interaction energy			-0.4 $\pm$ 0.1	5	-2.5 $\pm$ 0.2 <sup>†</sup>	5	-0.4 $\pm$ 0.1 <sup>†</sup>	5
$\beta$ 2-WT -active								
$\beta$ 2-H93 $\epsilon$ Nitrogen Solvation	34.8 $\pm$ 3.0	5	18.9 $\pm$ 2.4*	5	29.9 $\pm$ 2.4	5	33.5 $\pm$ 3.0	5
$\beta$ 2-H93 D192 Water-bridge	23.5 $\pm$ 3.1	5	18.7 $\pm$ 2.1	5	21.8 $\pm$ 1.1	5	26.6 $\pm$ 2.7	5
$\beta$ 2-H93 LIG Electrostatic energy			-1.0 $\pm$ 0.2	5	-0.1 $\pm$ 0.2 <sup>†</sup>	5	0.5 $\pm$ 0.1 <sup>†</sup>	5



β2-H93 LIG Van der Waals energy			-1.8 ± 0.2	5	-0.8 ± 0.1	5	-0.6 ± 0.1	5
β2-H93 LIG Interaction energy			-2.8 ± 0.2	5	-0.9 ± 0.1 <sup>†</sup>	5	-0.1 ± 0.2 <sup>†</sup>	5
β1-WT active vs β2-WT active energy			2.4 <sup>#</sup>		-1.6 <sup>#</sup>		-0.3	

\*p<0.05 compared with the values obtained from the apo unbound structure using an unpaired t-test.

#p<0.05 comparing the interaction energy between β1 and β2

<sup>†</sup>p<0.05 comparing values between ICI89406 and ICI89406np for the β1-WT or β2-WT

Table 4.

Table of interaction energies, solvation, and water-bridges of ligand and important residues calculated from MD simulations for ligands examined in the inactive structures. Numerical values are calculated as percentage of frames (for nitrogen solvation and water bridge formation) and the interaction energy is given in kcal/mol. Values are mean  $\pm$  sem of n separate determination. Compounds are compared with values obtained in the unbound (*apo*) structure using an unpaired t-test. The difference in the interaction energy to I118/H93 is also given between the compound binding to the  $\beta$ 1-WT and  $\beta$ 2-WT and compared using an unpaired t-test. Full details of each replicate, and all p values are given in Supp. Table 1-4.

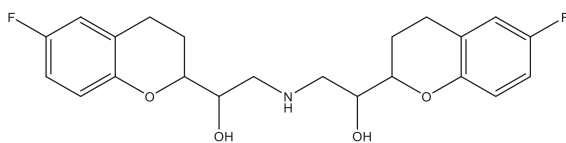
	Unbound <i>apo</i>	n	xamoterol	n	ICI89406	n	ICI89406np	n	betaxolol	n	bisoprolol	n	esmolol	n
$\beta$ 1-WT-inactive														
$\beta$ 1-I118 LIG electrostatic energy			0.9 $\pm$ 0.1	5	0.3 $\pm$ 0.1 <sup>†</sup>	5	0.1 $\pm$ 0.0 <sup>†</sup>	5	0.7 $\pm$ 0.0	5	0.7 $\pm$ 0.1	5	0.6 $\pm$ 0.0	5
$\beta$ 1-I118 LIG Van der Waals energy			-1.6 $\pm$ 0.1	5	-2.5 $\pm$ 0.3 <sup>†</sup>	5	-0.6 $\pm$ 0.1 <sup>†</sup>	5	-0.06 $\pm$ 0.01	5	-0.09 $\pm$ 0.03	5	-0.05 $\pm$ 0.01	5
$\beta$ 1-I118 LIG Interaction energy			-0.7 $\pm$ 0.1	5	-2.1 $\pm$ 0.3 <sup>†</sup>	5	-0.5 $\pm$ 0.1 <sup>†</sup>	5	0.6 $\pm$ 0.0	5	0.7 $\pm$ 0.1	5	0.6 $\pm$ 0.0	5
$\beta$ 2-WT-inactive														
$\beta$ 2-H93 $\epsilon$ Nitrogen Solvation	41.2 $\pm$ 1.2	5	24.4 $\pm$ 5.2*	5	11.0 $\pm$ 3.2*	5	27.9 $\pm$ 6.6	5	40.8 $\pm$ 4.1	5	36.8 $\pm$ 4.9	5	39.4 $\pm$ 2.0	5
$\beta$ 2-H93 D192 Water-bridge	20.3 $\pm$ 3.4	5	16.4 $\pm$ 4.1	5	2.1 $\pm$ 1.8* <sup>†</sup>	5	21.4 $\pm$ 6.3 <sup>†</sup>	5	15.3 $\pm$ 4.1	5	19.2 $\pm$ 5.2	5	31.0 $\pm$ 1.5*	5
$\beta$ 2-H93 LIG Electrostatic energy			-1.3 $\pm$ 0.2	5	0.5 $\pm$ 0.3	5	0.3 $\pm$ 0.1	5	0.2 $\pm$ 0.2	5	0.3 $\pm$ 0.2	5	0.4 $\pm$ 0.1	5
$\beta$ 2-H93 LIG Van der Waals energy			-1.6 $\pm$ 0.1	5	-2.4 $\pm$ 0.4 <sup>†</sup>	5	-0.3 $\pm$ 0.1 <sup>†</sup>	5	-0.1 $\pm$ 0.0	5	-0.1 $\pm$ 0.0	5	-0.1 $\pm$ 0.0	5
$\beta$ 2-H93 LIG Interaction energy			-2.9 $\pm$ 0.3	5	-1.9 $\pm$ 0.7 <sup>†</sup>	5	0.0 $\pm$ 0.0 <sup>†</sup>	5	0.2 $\pm$ 0.2	5	0.2 $\pm$ 0.1	5	0.4 $\pm$ 0.1	5
$\beta$ 1-WT inactive vs $\beta$ 2-WT energy inactive			2.1#		-0.2		-0.5#		0.4		0.4#		0.2	

\*p<0.05 compared with the values obtained from the apo unbound structure using an unpaired t-test.

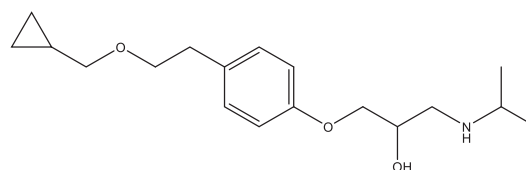
#p<0.05 comparing the interaction energy between  $\beta 1$  and  $\beta 2$

†p,0.05 comparing values between ICI89406 and ICI89406np for the  $\beta 1$ -WT /  $\beta 2$ -WT

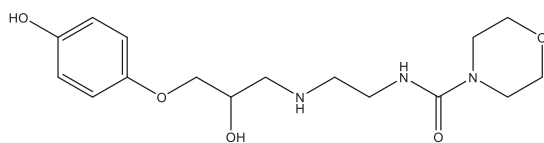
Figure 1



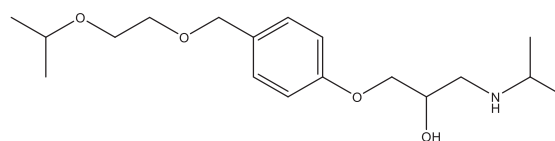
nebivolol



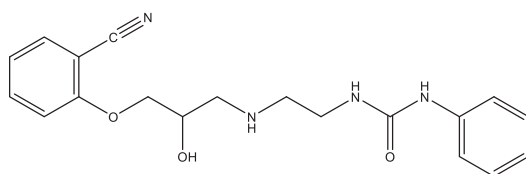
betaxolol



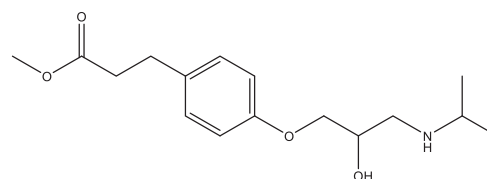
xamoterol



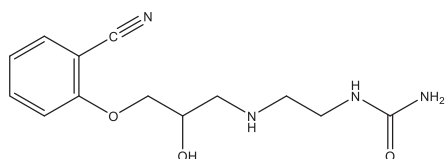
bisoprolol



ICI89406



esmolol



ICI89406np

Figure 2

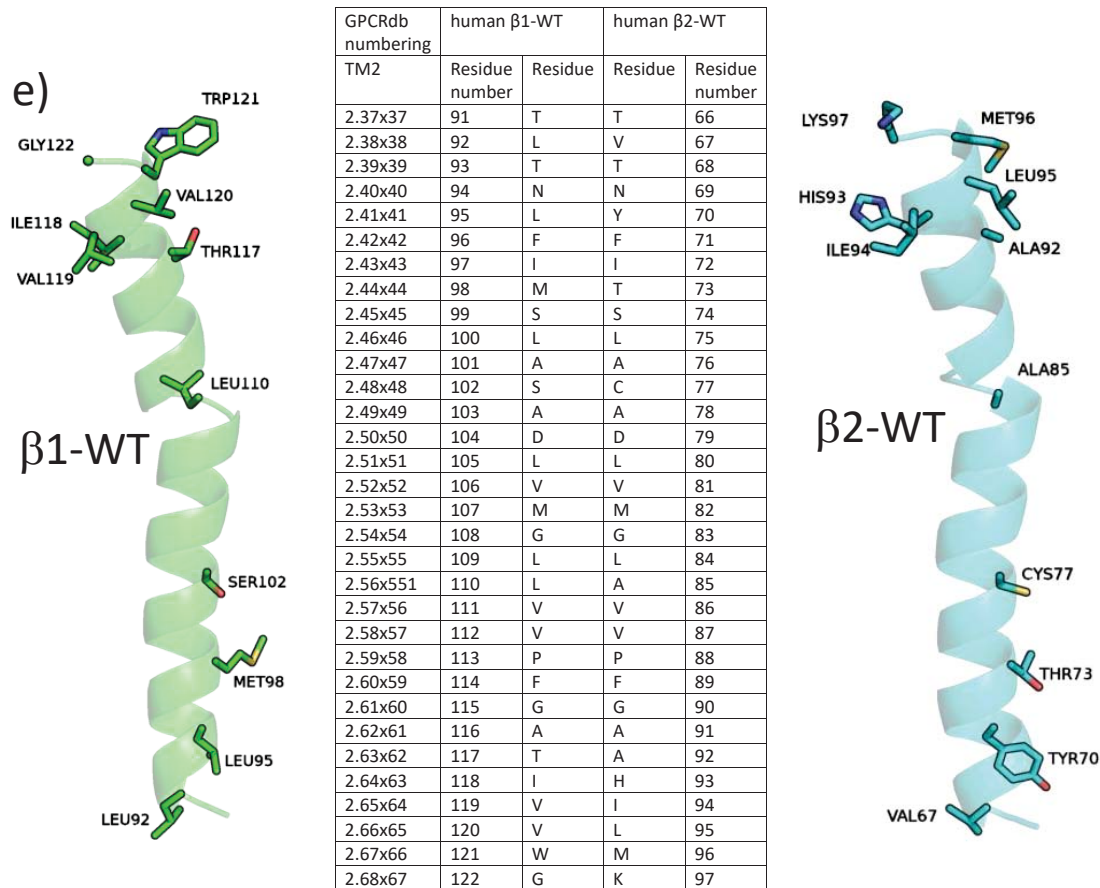
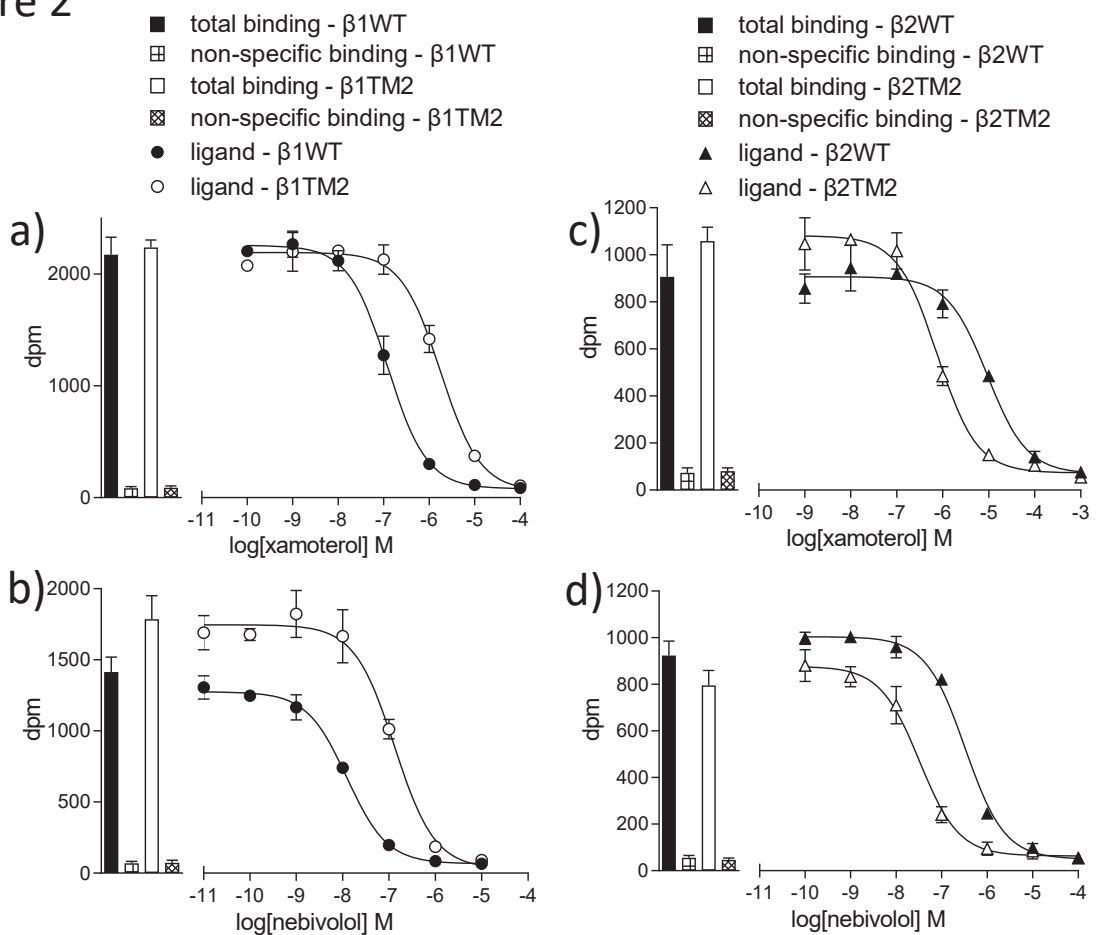


Figure 3

●  $\beta$ 1-AR  
○  $\beta$ 2-AR  
▲  $\beta$ 1-I118H

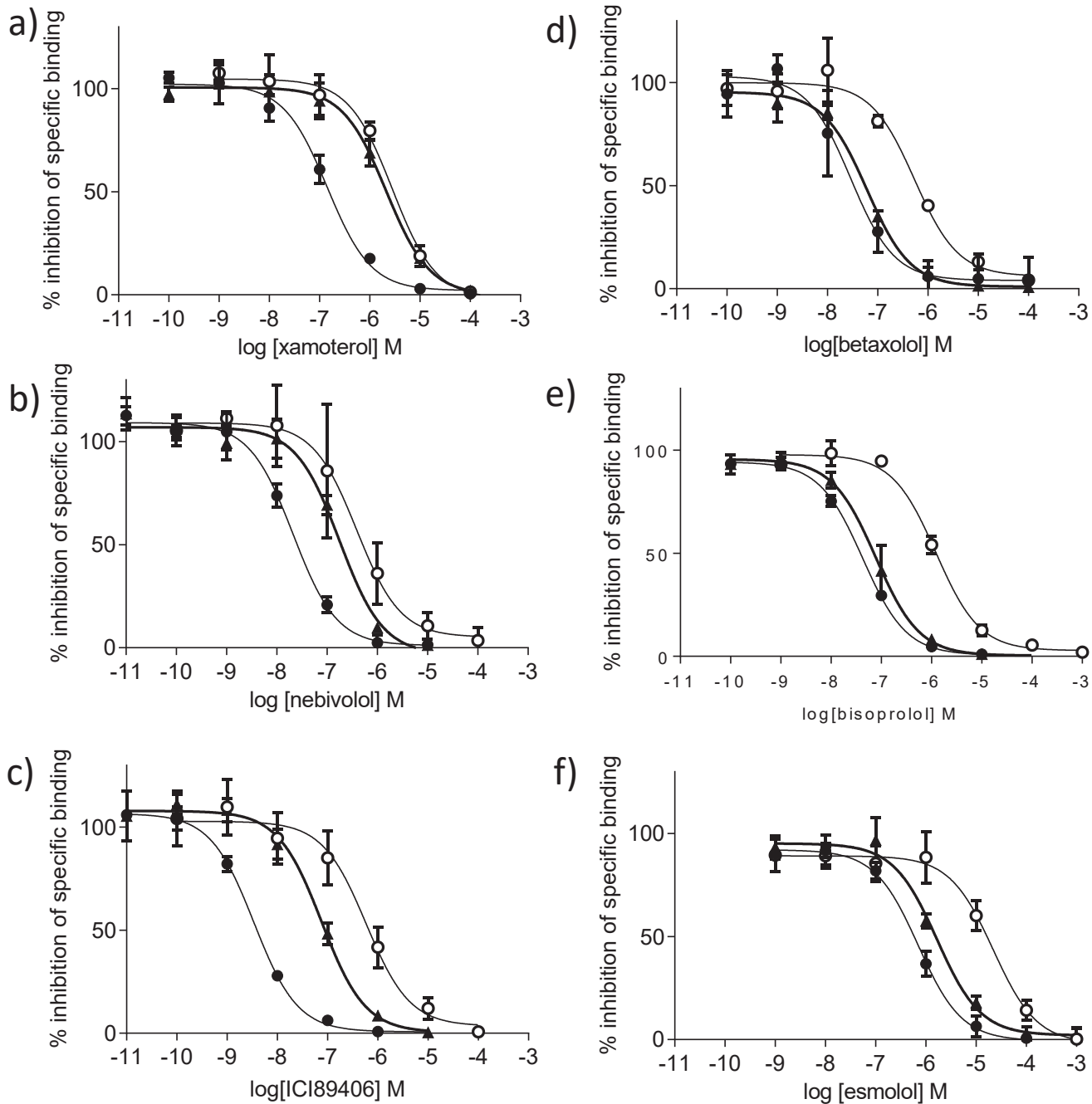


Figure 4

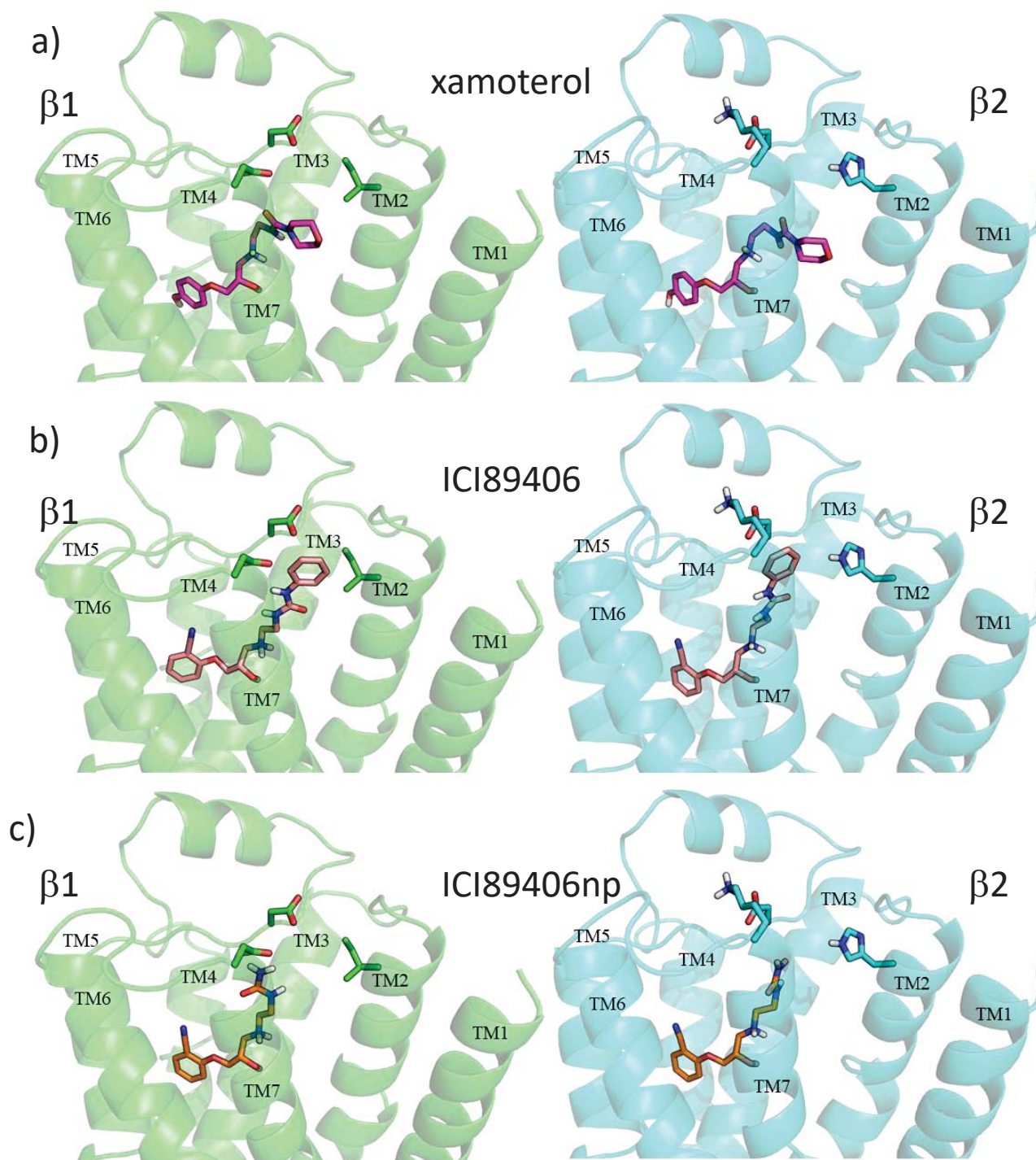


Figure 5

